Neurogenetics (2025) 26:82
https://doi.org/10.1007/s10048-025-00864-1

RESEARCH

# Missense variants in PKAN: insights from a multi-patient genetic analysis

Melisa Kılıç[1,2] · Sevcan Mercan[3] · Banu Özen Barut[4] · Duruhan Meltem Demirkıran[5] · Gül Yalçın Çakmaklı[6] · Nihan Hande Akçakaya[7] · Kanay Yararbaş[8] · Omer Faruk Duzenli[9,10] · Murat Gültekin[11] · Zuhal Yapıcı[12] · Sibel Aylin Uğur İşeri[1]

Received: 17 September 2025 / Accepted: 29 October 2025
© The Author(s), under exclusive licence to Springer-Verlag GmbH Germany, part of Springer Nature 2025

## Abstract

Pantothenate kinase-associated neurodegeneration (PKAN) is a common subtype of neurodegeneration with brain iron accumulation (NBIA), caused by biallelic variants in the *PANK2* gene. In this study, we investigated five unrelated patients clinically suspected of PKAN (four atypical, one classical) using next-generation sequencing followed by Sanger confirmation and segregation analysis where appropriate. We identified five distinct missense variants, including one novel association, all occurring in biallelic states. Notably, two patients carried the same homozygous variant (ENST00000610179.7:c.503G>T), previously associated with atypical PKAN, which may suggest either an elevated local carrier frequency or an unrecognized founder effect. The ENST00000610179.7:c.1253C>T; p.(Thr418Met) variant, identified in a patient with late-onset PKAN, has previously been reported in both classical and atypical forms of the disease, suggesting that residual enzyme activity may contribute to the observed phenotypic variability. To evaluate the impact of missense variants, we employed DynaMut2 and AlphaMissense. Two variants were predicted to be structurally destabilizing and pathogenic, while others showed neutral or conflicting predictions. Our findings highlight the complexity of interpreting missense variants in PKAN and support the utility of combining in silico predictions with detailed genotype–phenotype correlations. Although no consistent pattern was observed across all prediction tools and clinical outcomes, this study contributes to the expanding mutational spectrum of *PANK2* and emphasizes the need for further functional validation to improve diagnostic accuracy in NBIA disorders.

**Keywords** PKAN · PANK2 · Missense variants · NBIA

## Introduction

Neurodegeneration with brain iron accumulation (NBIA) encompasses a group of rare, progressive neurodegenerative disorders characterized by abnormal brain iron deposition in the brain, leading to dysregulated metabolism. These conditions result from pathogenic variations in multiple genes, predominantly following an autosomal recessive inheritance pattern, though X-linked dominant and autosomal dominant forms have also been identified [1]. NBIA includes several distinct subtypes, such as Pantothenate kinase-associated neurodegeneration (PKAN), phospholipase A2-associated neurodegeneration, beta-propeller protein-associated neurodegeneration, mitochondrial membrane protein-associated neurodegeneration, fatty acid hydroxylase-associated neurodegeneration, coenzyme-A synthase protein-associated neurodegeneration, neuroferritinopathy, aceruloplasminemia, Woodhouse-Sakati syndrome, and Kufor-Rakeb syndrome [2].

PKAN, the most common form of NBIA, is marked by excessive iron accumulation in the brain, particularly in the

Melisa Kılıç and Sevcan Mercan contributed equally.

Melisa Kılıç, Banu Özen Barut, Duruhan Meltem Demirkıran, Gül Yalçın Çakmaklı, Nihan Hande Akçakaya, Murat Gültekin, Zuhal Yapıcı, and Sibel Aylin Uğur İşeri Turkish NBIA Study Group

Extended author information available on the last page of the article

Published online: 25 November 2025

globus pallidus and substantia nigra [3]. It is caused by biallelic pathogenic variants in the *PANK2* gene, which encodes pantothenate kinase 2, a mitochondrial enzyme responsible for catalyzing the first step of the Coenzyme A (CoA) biosynthetic pathway [3, 4]. Impaired *PANK2* activity leads to diminished CoA levels, resulting in mitochondrial dysfunction, cytosolic iron deposition, oxidative stress and neurotoxicity [3, 4]. Advances in next-generation sequencing (NGS) have significantly improved the ability to diagnose NBIA disorders, including PKAN, by facilitating the rapid identification of causative variations across complex phenotypes and multiple genes [5].

PKAN manifests in two clinical subtypes: (i) Classical PKAN: Early-onset, typically emerging in the first decade of life, characterized by rapidly progressing dystonia, dysarthria, and rigidity. (ii) Atypical PKAN: Later-onset with a more gradual progression, often manifesting psychiatric symptoms during the second decade [4]. However, certain cases displaying overlapping or atypical features could not be clearly assigned to either group and were therefore referred to as "intermediate" PKAN [4].

This study aims to further elucidate the genetic basis of PKAN by analyzing five individuals who were clinically considered to have PKAN within the NBIA spectrum but lacked molecular confirmation prior to this study. Genetic analysis was performed using NGS; followed by Sanger sequencing for familial segregation analysis in two cases to confirm compound heterozygosity. The study identifies five distinct PKAN-associated variants in five unrelated individuals, including one variant newly associated with PKAN. These findings contribute to the expanding genetic landscape of PKAN, offering insights that may inform future diagnostic and therapeutic strategies.

## Materials and methods

### Patient recruitment

Five unrelated patients clinically suspected of having PKAN (four atypical, one typical) were enrolled to investigate the underlying genetic causes. Written informed consent was obtained from all participants and available family members in accordance with the ethical guidelines of the Istanbul University, Istanbul Faculty of Medicine Clinical Ethics Committee. Detailed clinical information for the five patients included in this study is presented in Table 1, summarizing the key neurological features, disease course, and classification as classical or atypical PKAN.

## Genetic analysis

To identify causative variants, targeted Clinical Exome Sequencing (CES) or Whole Exome Sequencing (WES) was performed. Cases 1 and 2 underwent CES v3, case 3 underwent CES v2, while cases 4 and 5 were analyzed by WES. CES (v2 or v3, SOPHiA Genetics, Lausanne, Switzerland) targets a curated set of clinically relevant genes, while WES captures nearly all protein coding regions of the genome.

**Table 1** Summary of clinical findings in five PKAN patients

| Case | Sex | Cons. | Onset/ current age | Initial symptom(s) | Main neurological findings | Clinical course | PKAN Class |
|---|---|---|---|---|---|---|---|
| 1 | F | Yes (1stCou) | 17y/39y | Gait disturbance | Dysarthria, cervical dystonia with retrocollis, jaw-opening dystonia, generalized dystonia with opisthotonic posturing | Progression to wheelchair dependence by age 29 | A |
| 2 | F | No | 6y/16y | Visual impairment (retinitis pigmentosa) | Severe generalized dystonia, jaw-closing dystonia, bradykinesia, brisk reflexes | Progression to wheelchair dependence by age 14 | C |
| 3 | M | Yes | 20y/23y | Speech and swallowing difficulties. Lumbar pain following a backward fall | Dysarthria, bilateral blepharospasm, jaw-opening dystonia, cervical and limb (right arm and leg) dystonia, bradykinesia, rigidity, postural instability | Progression to requiring assistance for ambulation by age 24 | A |
| 4 | M | Yes (1stCou) | 17y/37y | Gait disturbance | Spasmodic dysphonia, tongue dystonia, bilateral rigidity, bradykinesia, freezing of gait, mild ID | Slowly progressive with predominating psychiatric and parkinsonian features | A |
| 5 | M | Yes (2ndCou) | 23y/63y | Left foot dystonia | Hypophonic and dysarthric speech, facial hypomimia, bradykinesia, upward gaze limitation, tongue protrusion and jaw-closing dystonia, left food dystonia, postural instability, mild memory difficulty | Slow progression to requiring assistance for ambulation by age 59 | A |

Abbreviations: A: atypical PKAN, C: classical PKAN; Cons: parental consanguinity; Cou: cousin; F: female; ID: intellectual disability; M: male; y: year

Genomic DNA was extracted from peripheral blood using the QIAamp DNA Blood Maxi Kit (Qiagen GmbH, Hilden, Germany), following the manufacturer's protocol. For WES, exonic regions were captured using the SureSelect Human All Exon v6 kit (Agilent Technologies, Santa Clara, CA, USA) and sequenced on an Illumina NovaSeq platform.

## Bioinformatics and variant prioritization

Bioinformatic analysis was conducted using the SOPHiA DDM platform (SOPHiA Genetics SA, Switzerland). Variant annotation and prioritization were performed using the platform's proprietary software, focusing on NBIA-associated genes, especially *PANK2*. Variant visualization was carried out using Integrative Genomics Viewer (IGV). To ensure alignment with the hg38 genome build, BAM files from cases 3 to 5 originally mapped to hg19 were converted using the Liftover function in CrossMap software with the hg19ToHg38.over.chain file obtained from the UCSC Genome Browser [6]. (https://crossmap.readthedocs.io/en/latest/).

Variant pathogenicity assessment followed ACMG/AMP guidelines [7] using the GeneBe platform [8] for both the MANE Select (ENST00000610179.7) and the longest protein-coding (ENST00000316562.9) transcripts (GeneBe last accessed: 20 October 2025].

## Variant validation and annotation

*PANK2* variants were confirmed by Sanger sequencing when necessary, particularly to assess trans-segregation in compound heterozygous cases. Variants were annotated using both the MANE Select transcript (ENST00000610179.7; NM_001386393.1) and the longest protein-coding transcript (ENST00000316562.9; NM_153638.4; Q9BZ23). Throughout the manuscript, all variants both those identified in our study and those reported in the literature are described according to the MANE transcript, unless otherwise specified. Of note, the isoform encoded by the MANE transcript features a non-AUG start codon CUG, unlike the larger isoform. In the present report, whenever a variant is presented only at the protein level, it refers to the MANE transcript translation, with the corresponding change in the long isoform provided in square brackets. This approach facilitates comparison with previous reports, many of which annotate variants based on the long transcript.

Sanger sequencing data were analyzed using CLC Genomics Workbench v3.6.5 (CLC Bio, Aarhus, Denmark). To visualize missense variants, the Lollipops variant visualization tool was used to map their positions along the 570-residue PANK2 isoform (Q9BZ23) [9].

## Protein modeling and structural analysis

Protein structure information was obtained from AlphaFold2 (AF-Q9BZ23-F1-v4; full-length model). The potential impact of missense variants on protein stability was assessed using DynaMut2 Predicted changes in Gibbs Free Energy (ΔΔG) were considered destabilizing when below 0.0 kcal/mol [10].

Structural visualizations were generated via the DynaMut2 web interface only for variants predicted to be destabilizing and also classified as pathogenic by AlphaMissense [11].

## Results

Five patients clinically suspected of PKAN based on their characteristic neurological findings and MRI features were genetically analyzed in this study. Their clinical characteristics, including age at onset, main neurological manifestations, disease course, and classification as classical or atypical PKAN, are summarized in Table 1.

Clinically, the cohort comprised individuals with variable ages at onset ranging from childhood to early adulthood, reflecting both classical and atypical forms of PKAN. The single classical case (Case 2) presented with early-onset dystonia, gait disturbance, and rapid motor decline, while the remaining atypical cases exhibited later onset, slower disease progression, and predominant speech or oromandibular dystonia. Brain MRI in all five patients revealed the pathognomonic *"eye-of-the-tiger"* sign, characterized by central hyperintensity within the hypointense globus pallidus, confirming the diagnosis of PKAN.

In two families (Cases 1 and 3), affected siblings with similar phenotypes were also reported. The sister of Case 1 developed comparable dystonic and oromandibular symptoms at the age of 13 and died at 32 after a progressive disease course. In the family of Case 3, the proband's older sister presented at 16 years of age with speech and gait difficulties and is currently 29 years old with generalized dystonia and severe postural instability. Only the index patients were genetically analyzed in this study.

Using NGS, followed by Sanger sequencing for familial segregation analysis in two cases, we identified biallelic pathogenic or likely pathogenic variants in *PANK2* across all five PKAN individuals **(**Table 2 and Fig. 1**).** Copy number variation (CNV) analysis from NGS data was applicable

**Table 2** Variants identified in five PKAN patients with corresponding clinical classification, annotated according to both the longest protein-coding (ENST00000316562.9) and the MANE select (ENST00000610179.7) transcripts. GeneBe ACMG classifications were identical for both transcripts for each variant

| chr20 position (hg38) | Case | Zygo. | Consequence | PKAN Class | ACMG | AC | Clin-Var | SNP ID | Ex | HGVSc | HGVSp |
|---|---|---|---|---|---|---|---|---|---|---|---|
| 3,908,130-G-T | 3, 4 | hom, hom | missense | A, A | LP | 4 | NA | rs1348762206 | 2 | ENST00000316562.9:c.833G>T | p.Arg278Leu |
| | | | | | | | | | | ENST00000610179.7:c.503G>T | p.Arg168Leu |
| 3,910,722-C-T | 1 | het | missense | A | LP | 1 | NA | rs768909160 | 3 | ENST00000316562.9:c.1127 C>T | p.Pro376Leu |
| | | | | | | | | | | ENST00000610179.7:c.797 C>T | p.Pro266Leu |
| 3,912,634-G-A | 2 | het | missense, splice region | C | P | 1 | LP, P | rs137852963 | 4 | ENST00000316562.9:c.1412G>A | p.Ser471Asn |
| | | | | | | | | | | ENST00000610179.7:c.1082G>A | p.Ser361Asn |
| 3,917,016-T-C | 1, 2 | het, het | missense | A, C | P | 3 | P | rs775459398 | 5 | ENST00000316562.9:c.1502T>C | p.Ile501Thr |
| | | | | | | | | | | ENST00000610179.7:c.1172T>C | p.Ile391Thr |
| 3,918,717-C-T | 5 | hom | missense | A | P | 39 | P(5) | rs137852967 | 6 | ENST00000316562.9:c.1583 C>T | p.Thr528Met |
| | | | | | | | | | | ENST00000610179.7:c.1253 C>T | p.Thr418Met |

Abbreviations: A: atypical PKAN; AC: allele count from gnomAD v4.1.0; C: classical PKAN, Ex: exon number (out of 7 exons for both transcripts); HGVS: Human Genome Variation Society nomenclature for coding DNA (c) and protein (p) sequences; LP: likely pathogenic, NA: not available; P: pathogenic, Zygo: zygosity

only to Cases 1 and 2, and no CNVs were detected in NBIA-associated genes.

In Cases 1 and 2, CES identified potential compound heterozygous variants in *PANK2*: ENST00000610179.7:c.797C>T; p.(Pro266Leu) and c.1172T>C; p.(Ile391Thr) in Case 1, and c.1082G>A p.(Ser361Asn) and c.1172T>C; p.(Ile391Thr) in Case 2, the latter variant being shared between the two patients. Segregation analysis confirmed that the variants were in trans, thereby establishing true compound heterozygosity (Supplementary Fig. 1**).** Notably, Case 1 also harbored two heterozygous variants in *PLA2G6*; however, subsequent Sanger sequencing demonstrated that both were paternally inherited. Combined with phenotype correlation, these variants were regarded as clinically insignificant.

Cases 3 and 4 were identified with the same *PANK2* variant both in the homozygous state: ENST00000610179.7:c.503G>T; p.(Arg168Leu). Notably, these patients were recruited from different neurology departments at different times, and their samples were sequenced independently using CES and WES, respectively. Finally, case 5 carried a homozygous *PANK2* variant, ENST00000610179.7:c.1253C>T; p.(Thr418Met).

None of the variants identified in this study were found in the homozygous state in public databases, although they are present very rarely in the heterozygous state. All identified variants are localized to catalytic core region of the protein (Fig. 2a). To the best of our knowledge, ENST00000610179.7:c.797C>T; p.(Pro266Leu) in case 1 represents a novel association of this variant with the PKAN phenotype.

We analyzed the five identified missense variants using DynaMut2 to evaluate their potential impact on protein stability, and compared the results with pathogenicity predictions from AlphaMissense (Table 3). Among these, the p.Arg168Leu [p.Arg278Leu] and p.Ile391Thr [p.Ile501Thr] variants were predicted to be destabilizing ($\Delta\Delta G < 0$ kcal/mol) and were also classified as pathogenic by AlphaMissense. Accordingly, structural modeling showed that both variants are located in conserved regions of the PANK2 protein and may disrupt local structural integrity (Fig. 2b). The remaining three variants were either predicted to have neutral or stabilizing effects on protein structure and were not consistently classified as pathogenic.

## Discussion

In line with our findings, missense variants remain particularly challenging to interpret compared to loss-of-function (LoF) mutations, as their pathogenicity often stems from subtle alterations in protein structure or function rather than complete disruption. While LoF variants typically lead to a

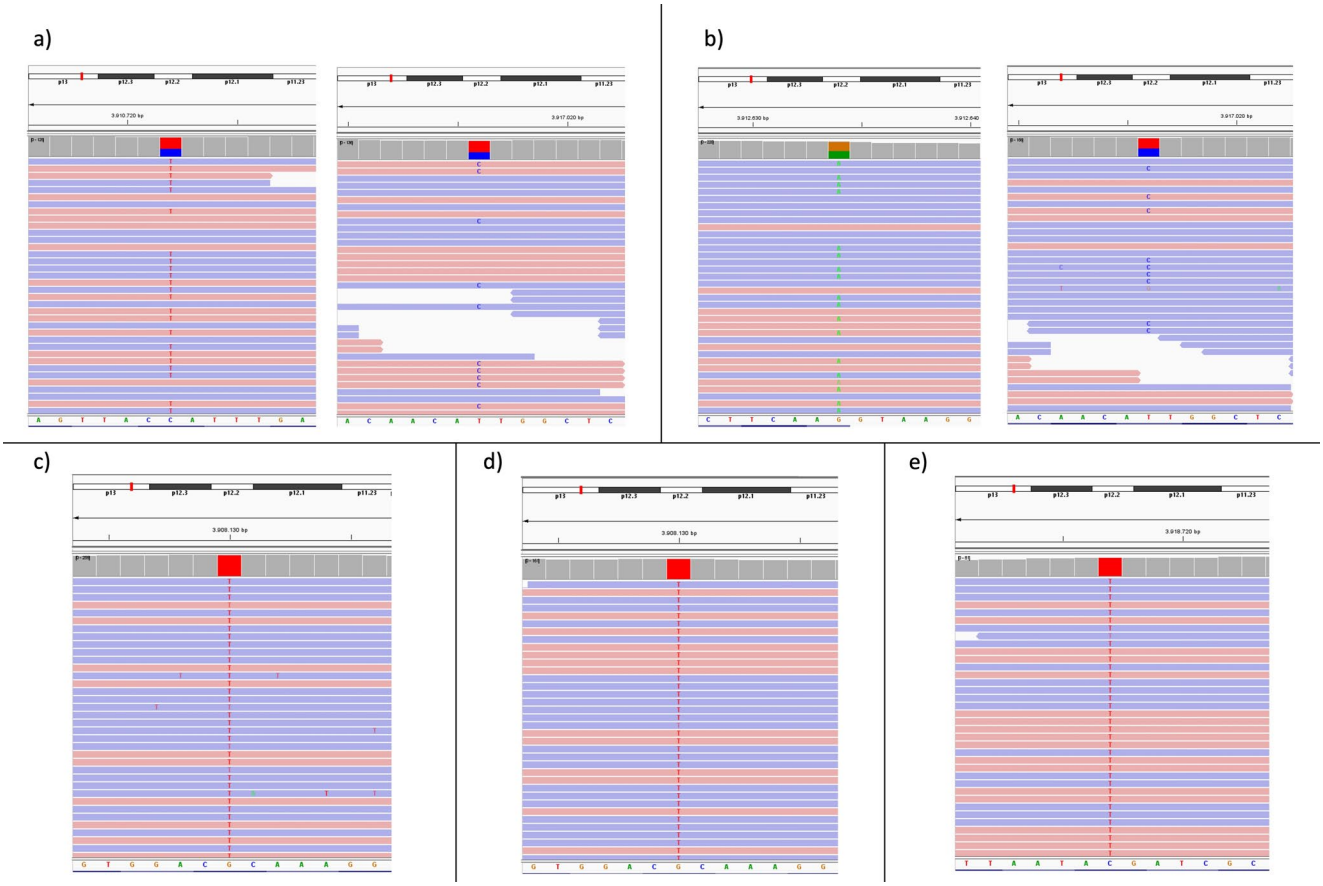



**Fig. 1** IGV (hg38) views of cases 1 to 5 (**a**–**e**). The first two cases (**a**, **b**) with compound heterozygous variants are shown with two panels each

clear loss of activity, missense changes require more comprehensive evaluation. In this context, in silico prediction tools and genotype–phenotype correlations are critical for assessing their clinical significance. Given this complexity, focused efforts to identify, characterize, and clinically interpret missense variants are essential for improving diagnostic precision and advancing personalized treatment approaches.

Atypical PKAN Case 1 and classical PKAN Case 2 were both found to be compound heterozygous, carrying the variants ENST00000610179.7:c.797C>T; p.(Pro266Leu)/ENST00000610179.7:c.1172T>C; p.(Ile391Thr) and ENST00000610179.7:c.1082G>A; p.(Ser361Asn)/ENST00000610179.7:c.1172T>C; p.(Ile391Thr), respectively. Thus, both cases share the ENST00000610179.7:c.1172T>C; p.(Ile391Thr) variant as one of their compound heterozygous alleles. The ENST00000610179.7:c.797C>T; p.(Pro266Leu) variant is clinically novel, whereas both ENST00000610179.7:c.1172T>C; p.(Ile391Thr) and ENST00000610179.7:c.1082G>A; p.(Ser361Asn) have previously been reported in compound heterozygous states; the former in a late-onset PKAN sibling pair [12] and the latter in an early-onset patient [13]. Notably, the G>A transition underlying the latter serine (Ser) to asparagine (Asn) substitution occurs at the last nucleotide of exon 4 (of a total of 7 exons) in both the long and MANE Select isoforms, suggesting a potential effect as a splice-site variant. If splicing is indeed affected, this change may result in a LoF consequence, which could account for the more severe, classical PKAN phenotype observed in our patient and in the previously reported case. Confirmation of this potential splicing effect would require RNA-level studies.

The ENST00000610179.7:c.503G>T; p.(Arg168Leu) variant was identified in the homozygous state in two atypical PKAN cases (Cases 3 and 4). This variant has previously been reported in a homozygous atypical PKAN patient [4], further supporting its pathogenic potential. In gnomAD v4.1.0, it is listed four times in the heterozygous state. Its relatively frequent detection in Türkiye may indicate an elevated local carrier frequency, with consanguineous marriages elevating the likelihood of homozygosity. Alternatively, the observation may reflect an unrecognized founder effect. Interestingly, homozygosity for this variant has also been associated with the classical form of PKAN [14].

The ENST00000610179.7:c.1253C>T; p.(Thr418Met) variant observed in Case 5 is relatively frequent among

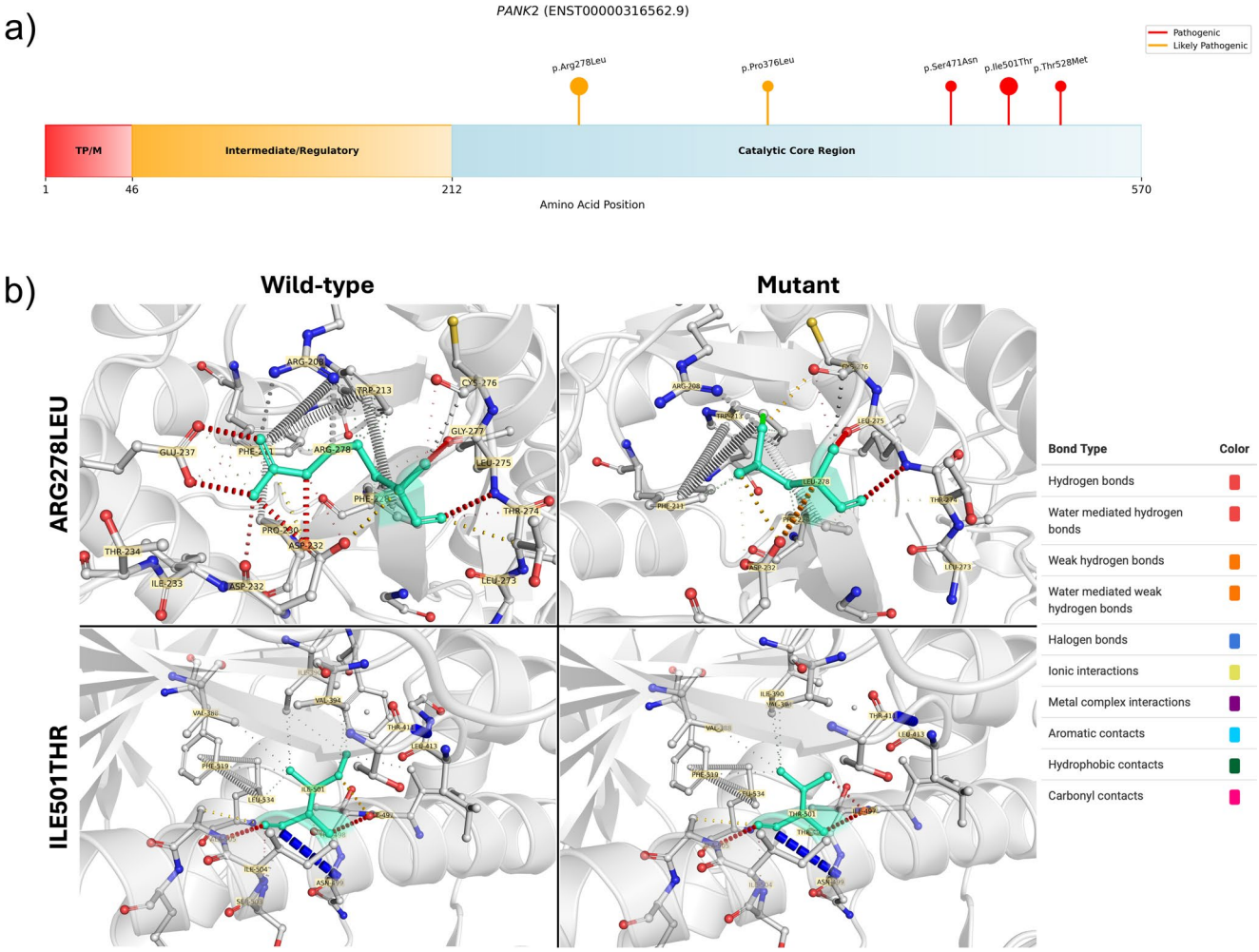



**Fig. 2** Schematic representation of missense variants identified in PANK2 and their predicted structural impact. (**a**) Missense variants detected in this study are mapped on the 570-residue PANK2 isoform (Q9BZ23) using Lollipops. Variants classified as pathogenic and likely pathogenic are indicated in red and yellow, respectively. Two variants, each identified in two unrelated cases, are represented with enlarged symbols. (**b**) Comparative structural modeling of selected variants using DynaMut2. The p.Arg278Leu substitution results in reduction of hydrogen bonds, suggesting potential structural destabilization and impaired enzymatic function. In contrast, the p.Ile501Thr substitution introduces novel intermolecular interactions, disrupting local hydrophobicity and potentially contributing conformational instability

**Table 3** Comparison of DynaMut2 and alphamissense (AM) predictions for the variants, based on the long isoform (Q9BZ23). Scores predicted as destabilizing by DynaMut2 or pathogenic by AM are highlighted in grey

| Q9BZ23 | Short isoform (MANE) | DynaMut2 ΔΔG kcal/mol | AM Pathogenity Score (Class) |
|---|---|---|---|
| p.Arg278Leu | p.Arg168Leu | −0.950 | 0.952 (LP) |
| p.Pro376Leu | p.Pro266Leu | 1.070 | 0.170 (LB) |
| p.Ser471Asn | p.Ser361Asn | 0.175 | 0.993 (LP) |
| p.Ile501Thr | p.Ile391Thr | −2.152 | 0.846 (LP) |
| p.Thr528Met | p.Thr418Met | 1.388 | 0.127 (LB) |

Abbreviations: AM: AlphaMissense; LB: Likely Benign; LP: Likely Pathogenic (LP)

PKAN patients [13]. It has been reported both in the compound heterozygous state—with other missense or truncating variants—and in the homozygous state, associated with a broad clinical spectrum and variable age of onset ranging from 2 to 25 years. Homozygous cases typically manifest later, between 17 and 25 years of age, and often exhibit a more atypical phenotype, as in our patient with disease onset at 23 years. Nevertheless, Werning et al., 2020 described two p.Thr418Met [p.Thr528Met] homozygous cases with classical and atypical PKAN diagnosis [14]. It is tempting to speculate that clinical severity may depend on the nature of the second allele in compound heterozygosity with this variant. For example, when paired with loss-of-function (LOF) variants such as ENST00000610179.7:c.243del; p.(Ser81ArgfsTer14) or ENST00000610179.7:c.1090_1096del; p.(Asn364Ter), onset occurred at 7 and 13 years, respectively. In contrast, when p.Thr418Met [p.Thr528Met] was combined with an in-frame deletion (ENST00000610

179.7:c.1112_1114del; p.(Arg371_Glu372delinsGln)), disease onset was as early as 2 years [13].

These observations underscore the importance of interpreting genetic variants in conjunction with clinical findings. The p.Thr418Met [p.Thr528Met] and p.Arg168Leu [p.Arg278Leu] variants have been associated with both classic and atypical PKAN phenotypes, suggesting that the clinical spectrum may be influenced by the range of residual *PANK2* activity [14]. This supports the notion that residual enzymatic function could serve as a modifier of disease severity in PKAN.

In rare disease research, functional validation of every missense variant is often impractical. Therefore, integrating clinical data with in silico predictions remains valuable for prioritizing variants. Although we used both DynaMut2 and AlphaMissense to assess structural impact and pathogenicity, a consistent correlation between predictions and clinical effect was not always observed. Differences between DynaMut2 and AlphaMissense predictions likely reflect the distinct principles of these tools: DynaMut2 estimates the energetic and conformational stability changes based on 3D structure, while AlphaMissense predicts pathogenicity from sequence conservation patterns learned from population-scale data. These findings reflect the necessity for cautious interpretation and further functional studies.

**Supplementary Information** The online version contains supplementary material available at https://doi.org/10.1007/s10048-025-00864-1.

**Acknowledgements** We thank the patients and their families for their participation and valuable contributions to this study. We sincerely thank the patients and their families for their participation and valuable contributions to this study. This research was supported by the Scientific Research Projects Coordination Unit of Istanbul University (Project Numbers: TYL-2024-40633, TSA-2024-40461 and TSA-2018-27512) and the ISTisNA Project (ISTKA No: TR10/22/THN). MK was a fellow of the TÜBİTAK 2210-A program and the ISTisNA Project. SAUI gratefully acknowledges the Turkish Academy of Sciences for the 2019 Distinguished Young Scientist Award (TÜBA-GEBİP).

**Author contributions** ZY and SAUI conceived and designed the study. ZY and SAUI also provided critical revisions of the manuscript. MK and SM performed the laboratory experiments, including DNA extraction and validation assays. MK and SM also conducted the bioinformatics analyses, variant annotation, data interpretation, and prepared the draft manuscript. HA and KY were involved in NGS analysis. MK and OFD performed in silico protein predictions. BOB, DMD, GYC, HA, MG, and ZY were responsible for patient recruitment, clinical evaluation, and collection of clinical data. All authors contributed to the drafting and editing of the manuscript, and all authors read and approved the final version.

**Funding** This research was supported by the Scientific Research Projects Coordination Unit of Istanbul University (Project Numbers: TYL-2024-40633, TSA-2024-40461 and TSA-2018-27512) and the ISTisNA Project (ISTKA No: TR10/22/THN).

**Data availability** No datasets were generated or analysed during the current study.

## Declarations

**Competing interests** The authors declare no competing interests.

## References

1. Hayflick SJ, Kurian MA, Hogarth P (2018) Neurodegeneration with brain iron accumulation. Handb Clin Neurol 147:293–305
2. Salomão RP et al (2016) A diagnostic approach for neurodegeneration with brain iron accumulation: clinical features, genetics and brain imaging. Arq Neuropsiquiatr 74(7):587–596
3. Hayflick SJ, Jeong SY, Sibon OCM (2022) PKAN pathogenesis and treatment. Mol Genet Metab 137(3):283–291
4. Akcakaya NH et al (2017) Clinical and genetic features of PKAN patients in a tertiary centre in Turkey. Clin Neurol Neurosurg 154:34–42
5. Si L et al (2023) Novel mutations and molecular pathways identified in patients with brain iron accumulation disorders. Neurogenetics 24(4):231–241
6. Zhao H et al (2013) Crossmap: a versatile tool for coordinate conversion between genome assemblies. Bioinformatics 30(7):1006–1007
7. Richards S et al (2015) Standards and guidelines for the interpretation of sequence variants: a joint consensus recommendation of the American college of medical genetics and genomics and the association for molecular pathology. Genet Med 17(5):405–424
8. Stawiński P, Płoski R (2024) Genebe.net: implementation and validation of an automatic ACMG variant pathogenicity criteria assignment. Clin Genet 106(2):119–126
9. Jay JJ, Brouwer C (2016) Lollipops in the clinic: information dense mutation plots for precision medicine. PLoS One 11(8):e0160519
10. Intharanut K et al (2024) Identification of two novel variants, c.–35A>T and c.[–35A>T, 725T>G], in the FUT1 gene in a patient exhibiting the para-Bombay phenotype. Transfusion 64(12):2252–2259
11. Tordai H et al (2024) Analysis of alphamissense data in different protein groups and structural context. Sci Data 11(1):495
12. Molinuevo JL et al (2003) Pure akinesia: an unusual phenotype of Hallervorden-Spatz syndrome. Mov Disord 18(11):1351–1353
13. Hartig MB et al (2006) Genotypic and phenotypic spectrum of PANK2 mutations in patients with neurodegeneration with brain iron accumulation. Ann Neurol 59(2):248–256
14. Werning M et al (2020) PKAN neurodegeneration and residual PANK2 activities in patient erythrocytes. Ann Clin Transl Neurol 7(8):1340–1351

**Publisher's note** Springer Nature remains neutral with regard to jurisdictional claims in published maps and institutional affiliations.

Springer Nature or its licensor (e.g. a society or other partner) holds exclusive rights to this article under a publishing agreement with the author(s) or other rightsholder(s); author self-archiving of the accepted manuscript version of this article is solely governed by the terms of such publishing agreement and applicable law.

## Authors and Affiliations

**Melisa Kılıç[1,2] · Sevcan Mercan[3] · Banu Özen Barut[4] · Duruhan Meltem Demirkıran[5] · Gül Yalçın Çakmaklı[6] · Nihan Hande Akçakaya[7] · Kanay Yararbaş[8] · Omer Faruk Duzenli[9,10] · Murat Gültekin[11] · Zuhal Yapıcı[12] · Sibel Aylin Uğur İşeri[1]**

✉ Zuhal Yapıcı
zyapici@istanbul.edu.tr

✉ Sibel Aylin Uğur İşeri
sibel.ugur@istanbul.edu.tr

1 Department of Genetics, Aziz Sancar Institute of Experimental Medicine, Istanbul University, Istanbul, Türkiye

2 Graduate School of Health Sciences, Istanbul University, Istanbul, Türkiye

3 Department of Medical Genetics, Kafkas University Faculty of Medicine, Kars, Türkiye

4 Department of Neurology, Kartal Training and Research Hospital, Istanbul, Türkiye

5 Department of Neurology, Çukurova University Faculty of Medicine, Adana, Türkiye

6 Department of Neurology, Hacettepe University Faculty of Medicine, Ankara, Türkiye

7 Council of Forensic Medicine, Ministry of Justice, Istanbul, Türkiye

8 Department of Medical Genetics, Demiroglu Bilim University, Faculty of Medicine, Istanbul, Türkiye

9 Department of Neuroscience, Institute of Neurological Sciences, Istanbul University-Cerrahpaşa, Istanbul, Türkiye

10 Department of Neurogenetics, Institute of Neurological Sciences, Istanbul University-Cerrahpaşa, Istanbul, Türkiye

11 Department of Neurology, Erciyes University Faculty of Medicine, Kayseri, Türkiye

12 Department of Neurology, Istanbul University of Faculty Medicine, Istanbul, Türkiye